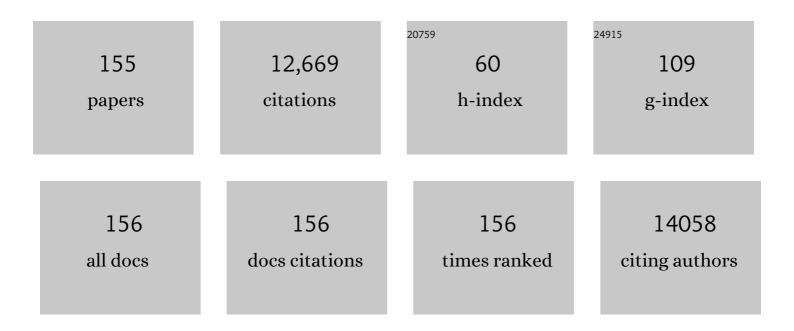
List of Publications by Year in descending order

Source: https://exaly.com/author-pdf/2601608/publications.pdf Version: 2024-02-01



#	Article	IF	CITATIONS
1	Surface modification of TiO2 photocatalyst for environmental applications. Journal of Photochemistry and Photobiology C: Photochemistry Reviews, 2013, 15, 1-20.	5.6	858
2	Effects of Single Metal-Ion Doping on the Visible-Light Photoreactivity of TiO ₂ . Journal of Physical Chemistry C, 2010, 114, 783-792.	1.5	685
3	Effects of TiO2 Surface Fluorination on Photocatalytic Reactions and Photoelectrochemical Behaviors. Journal of Physical Chemistry B, 2004, 108, 4086-4093.	1.2	591
4	Photoinduced charge transfer processes in solar photocatalysis based on modified TiO ₂ . Energy and Environmental Science, 2016, 9, 411-433.	15.6	494
5	Effects of the preparation method of the ternary CdS/TiO2/Pt hybrid photocatalysts on visible light-induced hydrogen production. Journal of Materials Chemistry, 2008, 18, 2379.	6.7	370
6	Carbon-doped TiO2 photocatalyst synthesized without using an external carbon precursor and the visible light activity. Applied Catalysis B: Environmental, 2009, 91, 355-361.	10.8	351
7	Treatment technologies for aqueous perfluorooctanesulfonate (PFOS) and perfluorooctanoate (PFOA). Frontiers of Environmental Science and Engineering in China, 2009, 3, 129-151.	0.8	344
8	Photocatalytic Comparison of TiO ₂ Nanoparticles and Electrospun TiO ₂ Nanofibers: Effects of Mesoporosity and Interparticle Charge Transfer. Journal of Physical Chemistry C, 2010, 114, 16475-16480.	1.5	330
9	Light-harvesting multi-walled carbon nanotubes and CdS hybrids: Application to photocatalytic hydrogen production from water. Energy and Environmental Science, 2011, 4, 685-694.	15.6	259
10	Reductive Defluorination of Aqueous Perfluorinated Alkyl Surfactants: Effects of Ionic Headgroup and Chain Length. Journal of Physical Chemistry A, 2009, 113, 690-696.	1.1	251
11	Sonochemical Degradation of Perfluorooctane Sulfonate (PFOS) and Perfluorooctanoate (PFOA) in Landfill Groundwater: Environmental Matrix Effects. Environmental Science & Technology, 2008, 42, 8057-8063.	4.6	231
12	Investigation on TiO2-coated optical fibers for gas-phase photocatalytic oxidation of acetone. Applied Catalysis B: Environmental, 2001, 31, 209-220.	10.8	206
13	Photosynthesis of formate from CO ₂ and water at 1% energy efficiency via copper iron oxide catalysis. Energy and Environmental Science, 2015, 8, 2638-2643.	15.6	204
14	Kinetics and Mechanism of the Sonolytic Conversion of the Aqueous Perfluorinated Surfactants, Perfluorooctanoate (PFOA), and Perfluorooctane Sulfonate (PFOS) into Inorganic Products. Journal of Physical Chemistry A, 2008, 112, 4261-4270.	1.1	203
15	Photoelectrochemical Investigation on Electron Transfer Mediating Behaviors of Polyoxometalate in UV-Illuminated Suspensions of TiO2and Pt/TiO2. Journal of Physical Chemistry B, 2003, 107, 3885-3890.	1.2	197
16	Strategic Modification of BiVO ₄ for Improving Photoelectrochemical Water Oxidation Performance. Journal of Physical Chemistry C, 2013, 117, 9104-9112.	1.5	191
17	Effect of the Anchoring Group in Ruâ^'Bipyridyl Sensitizers on the Photoelectrochemical Behavior of Dye-Sensitized TiO2Electrodes:Â Carboxylate versus Phosphonate Linkages. Journal of Physical Chemistry B, 2006, 110, 8740-8749.	1.2	188
18	Photocatalytic Reactivities of Nafion-Coated TiO2 for the Degradation of Charged Organic Compounds under UV or Visible Light. Journal of Physical Chemistry B, 2005, 109, 11667-11674.	1.2	187

#	Article	IF	CITATIONS
19	Visible light and Fe(III)-mediated degradation of Acid Orange 7 in the absence of H2O2. Journal of Photochemistry and Photobiology A: Chemistry, 2003, 159, 241-247.	2.0	184
20	Solar Hydrogen Production Coupled with the Degradation of a Dye Pollutant Using TiO ₂ Modified with Platinum and Nafion. International Journal of Photoenergy, 2014, 2014, 1-9.	1.4	172
21	Ultra-efficient and durable photoelectrochemical water oxidation using elaborately designed hematite nanorod arrays. Nano Energy, 2017, 39, 211-218.	8.2	171
22	Selective Photocatalytic Oxidation of NH3to N2on Platinized TiO2in Water. Environmental Science & Technology, 2002, 36, 5462-5468.	4.6	168
23	Solar water oxidation using nickel-borate coupled BiVO4 photoelectrodes. Physical Chemistry Chemical Physics, 2013, 15, 6499.	1.3	156
24	Sonochemical Degradation of Perfluorooctane Sulfonate (PFOS) and Perfluorooctanoate (PFOA) in Groundwater: Kinetic Effects of Matrix Inorganics. Environmental Science & Technology, 2010, 44, 445-450.	4.6	153
25	Photoelectrochemical Approach for Metal Corrosion Prevention Using a Semiconductor Photoanode. Journal of Physical Chemistry B, 2002, 106, 4775-4781.	1.2	152
26	Photocatalytic conversion of benzene to phenol using modified TiO2 and polyoxometalates. Catalysis Today, 2005, 101, 291-297.	2.2	152
27	Electrochemical Water Splitting Coupled with Organic Compound Oxidation: The Role of Active Chlorine Species. Journal of Physical Chemistry C, 2009, 113, 7935-7945.	1.5	148
28	Reversing CdS Preparation Order and Its Effects on Photocatalytic Hydrogen Production of CdS/Pt-TiO ₂ Hybrids Under Visible Light. Journal of Physical Chemistry C, 2011, 115, 6141-6148.	1.5	126
29	Comparative Study of Homogeneous and Heterogeneous Photocatalytic Redox Reactions:Â PW12O403-vs TiO2. Journal of Physical Chemistry B, 2004, 108, 6402-6411.	1.2	120
30	Sonochemical Degradation of Perfluorooctanesulfonate in Aqueous Film-Forming Foams. Environmental Science & Technology, 2010, 44, 432-438.	4.6	114
31	Boosting the electrocatalytic activities of SnO2 electrodes for remediation of aqueous pollutants by doping with various metals. Applied Catalysis B: Environmental, 2012, 111-112, 317-325.	10.8	111
32	Solar desalination coupled with water remediation and molecular hydrogen production: a novel solar water-energy nexus. Energy and Environmental Science, 2018, 11, 344-353.	15.6	111
33	New nanoporous carbon materials with high adsorption capacity and rapid adsorption kinetics for removing humic acids. Microporous and Mesoporous Materials, 2003, 58, 131-135.	2.2	108
34	Activation of Hematite Photoanodes for Solar Water Splitting: Effect of FTO Deformation. Journal of Physical Chemistry C, 2015, 119, 3810-3817.	1.5	108
35	Artificial Photosynthesis of C1–C3 Hydrocarbons from Water and CO ₂ on Titanate Nanotubes Decorated with Nanoparticle Elemental Copper and CdS Quantum Dots. Journal of Physical Chemistry A, 2015, 119, 4658-4666.	1.1	105
36	Organic dye-sensitized TiO2 as a versatile photocatalyst for solar hydrogen and environmental remediation. Applied Catalysis B: Environmental, 2012, 121-122, 206-213.	10.8	104

#	Article	IF	CITATIONS
37	Sn oupled pâ€&i Nanowire Arrays for Solar Formate Production from CO ₂ . Advanced Energy Materials, 2014, 4, 1301614.	10.2	96
38	A review on lithium recovery using electrochemical capturing systems. Desalination, 2021, 500, 114883.	4.0	96
39	Solar-Powered Electrochemical Oxidation of Organic Compounds Coupled with the Cathodic Production of Molecular Hydrogen. Journal of Physical Chemistry A, 2008, 112, 7616-7626.	1.1	89
40	Solar conversion of seawater uranium (VI) using TiO2 electrodes. Applied Catalysis B: Environmental, 2015, 163, 584-590.	10.8	87
41	Effects of electrolyte on the electrocatalytic activities of RuO2/Ti and Sb–SnO2/Ti anodes for water treatment. Applied Catalysis B: Environmental, 2010, 97, 135-141.	10.8	86
42	Visible-Light-Sensitized Production of Hydrogen Using Perfluorosulfonate Polymer-Coated TiO2Nanoparticles:Â An Alternative Approach to Sensitizer Anchoring. Langmuir, 2006, 22, 2906-2911.	1.6	82
43	Enhanced Photoelectrochemical Solar Water Splitting Using a Platinum-Decorated CIGS/CdS/ZnO Photocathode. ACS Applied Materials & Interfaces, 2015, 7, 21619-21625.	4.0	82
44	Electrolysis of urea and urine for solar hydrogen. Catalysis Today, 2013, 199, 2-7.	2.2	80
45	Effects of inorganic oxidants on kinetics and mechanisms of WO 3 -mediated photocatalytic degradation. Applied Catalysis B: Environmental, 2015, 162, 515-523.	10.8	79
46	Reductive degradation of perfluoroalkyl compounds with aquated electrons generated from iodide photolysis at 254 nm. Photochemical and Photobiological Sciences, 2011, 10, 1945-1953.	1.6	76
47	Preparation of ZnO nanorods by microemulsion synthesis and their application as a CO gas sensor. Sensors and Actuators B: Chemical, 2011, 160, 94-98.	4.0	75
48	Shift of the Reactive Species in the Sb–SnO ₂ -Electrocatalyzed Inactivation of <i>E. coli</i> and Degradation of Phenol: Effects of Nickel Doping and Electrolytes. Environmental Science & Technology, 2014, 48, 2877-2884.	4.6	74
49	A facile synthesis of CuFeO ₂ and CuO composite photocatalyst films for the production of liquid formate from CO ₂ and water over a month. Journal of Materials Chemistry A, 2017, 5, 2123-2131.	5.2	73
50	Photoelectrochemical performance of multi-layered BiOx–TiO2/Ti electrodes for degradation of phenol and production of molecular hydrogen in water. Journal of Hazardous Materials, 2012, 211-212, 47-54.	6.5	72
51	TiO2 complexed with dopamine-derived polymers and the visible light photocatalytic activities for water pollutants. Journal of Catalysis, 2017, 346, 92-100.	3.1	71
52	Solar-Powered Production of Molecular Hydrogen from Water. Journal of Physical Chemistry C, 2008, 112, 885-889.	1.5	70
53	Combinatorial doping of TiO ₂ with platinum (Pt), chromium (Cr), vanadium (V), and nickel (Ni) to achieve enhanced photocatalytic activity with visible light irradiation. Journal of Materials Research, 2010, 25, 149-158.	1.2	69
54	Photo-chargeable and dischargeable TiO2 and WO3 heterojunction electrodes. Applied Catalysis B: Environmental, 2012, 115-116, 74-80.	10.8	69

#	Article	IF	CITATIONS
55	Visible light photocatalytic activities of nitrogen and platinum-doped TiO2: Synergistic effects of co-dopants. Applied Catalysis B: Environmental, 2014, 147, 642-650.	10.8	69
56	Photoelectrochemical and Photocatalytic Behaviors of Hematite-Decorated Titania Nanotube Arrays: Energy Level Mismatch versus Surface Specific Reactivity. Journal of Physical Chemistry C, 2011, 115, 7134-7142.	1.5	66
57	Ag(I) ions working as a hole-transfer mediator in photoelectrocatalytic water oxidation on WO3 film. Nature Communications, 2020, 11, 967.	5.8	66
58	Synthesis of Al-doped ZnO Nanorods via Microemulsion Method and Their Application as a CO Gas Sensor. Journal of Materials Science and Technology, 2015, 31, 639-644.	5.6	65
59	Electrosprayed BiVO4 nanopillars coated with atomic-layer-deposited ZnO/TiO2 as highly efficient photoanodes for solar water splitting. Chemical Engineering Journal, 2018, 333, 721-729.	6.6	63
60	TiO ₂ Nanotube Array Photoelectrocatalyst and Ni–Sb–SnO ₂ Electrocatalyst Bifacial Electrodes: A New Type of Bifunctional Hybrid Platform for Water Treatment. ACS Applied Materials & Interfaces, 2015, 7, 1907-1914.	4.0	61
61	Sequential Combination of Electro-Fenton and Electrochemical Chlorination Processes for the Treatment of Anaerobically-Digested Food Wastewater. Environmental Science & Technology, 2017, 51, 10700-10710.	4.6	61
62	Direct In Situ Growth of Centimeterâ€Scale Multiâ€Heterojunction MoS ₂ /WS ₂ /WSe ₂ Thinâ€Film Catalyst for Photoâ€Electrochemical Hydrogen Evolution. Advanced Science, 2019, 6, 1900301.	5.6	60
63	Nanotextured Pillars of Electrosprayed Bismuth Vanadate for Efficient Photoelectrochemical Water Splitting. Langmuir, 2015, 31, 3727-3737.	1.6	59
64	Stand-alone photoconversion of carbon dioxide on copper oxide wire arrays powered by tungsten trioxide/dye-sensitized solar cell dual absorbers. Nano Energy, 2016, 25, 51-59.	8.2	58
65	How and to what extent do carbon materials catalyze solar hydrogen production from water?. Applied Catalysis B: Environmental, 2012, 125, 530-537.	10.8	52
66	A novel photoelectrochemical method of metal corrosion prevention using a TiO2 solar panel. Chemical Communications, 2001, , 281-282.	2.2	51
67	Photocatalytic conversion of carbon dioxide to methane on TiO2/CdS in aqueous isopropanol solution. Catalysis Today, 2016, 266, 153-159.	2.2	48
68	Dual modification of hematite photoanode by Sn-doping and Nb2O5 layer for water oxidation. Applied Catalysis B: Environmental, 2017, 201, 591-599.	10.8	47
69	Photocatalytic degradation of organic dye using titanium dioxide modified with metal and non-metal deposition. Materials Science in Semiconductor Processing, 2016, 41, 209-218.	1.9	46
70	Effects of TiO2 surface fluorination on photocatalytic degradation of methylene blue and humic acid. Research on Chemical Intermediates, 2010, 36, 127-140.	1.3	43
71	Shape-Dependent Charge Transfers in Crystalline ZnO Photocatalysts: Rods versus Plates. Journal of Physical Chemistry C, 2014, 118, 21331-21338.	1.5	43
72	A Composite Photocatalyst of CdS Nanoparticles Deposited on TiO2 Nanosheets. Journal of Nanoscience and Nanotechnology, 2006, 6, 3642-3646.	0.9	42

#	Article	IF	CITATIONS
73	Optical resonance and charge transfer behavior of patterned WO ₃ microdisc arrays. Energy and Environmental Science, 2016, 9, 3143-3150.	15.6	42
74	Template-engineered epitaxial BiVO ₄ photoanodes for efficient solar water splitting. Journal of Materials Chemistry A, 2017, 5, 18831-18838.	5.2	42
75	Rapid photocatalytic degradation of nitrobenzene under the simultaneous illumination of UV and microwave radiation fields with a TiO2 ball catalyst. Catalysis Today, 2018, 307, 65-72.	2.2	42
76	lonâ€Enhanced Conversion of CO ₂ into Formate on Porous Dendritic Bismuth Electrodes with High Efficiency and Durability. ChemSusChem, 2020, 13, 698-706.	3.6	42
77	Lithium ion-inserted TiO2 nanotube array photoelectrocatalysts. Applied Catalysis B: Environmental, 2013, 140-141, 233-240.	10.8	41
78	Nanotextured cupric oxide nanofibers coated with atomic layer deposited ZnO-TiO2 as highly efficient photocathodes. Applied Catalysis B: Environmental, 2017, 201, 479-485.	10.8	41
79	Titania nanofibers as a photo-antenna for dye-sensitized solar hydrogen. Photochemical and Photobiological Sciences, 2012, 11, 1437-1444.	1.6	40
80	Facilitating hole transfer on electrochemically synthesized p-type CuAlO ₂ films for efficient solar hydrogen production from water. Journal of Materials Chemistry A, 2017, 5, 10165-10172.	5.2	40
81	Electrocatalytic arsenite oxidation using iron oxyhydroxide polymorphs (α-, β-, and γ-FeOOH) in aqueous bicarbonate solution. Applied Catalysis B: Environmental, 2021, 283, 119608.	10.8	40
82	Study of special cases where the enhanced photocatalytic activities of Pt/TiO2 vanish under low light intensity. Catalysis Today, 2006, 111, 259-265.	2.2	39
83	Enhanced Solar Water Oxidation Performance of TiO ₂ via Band Edge Engineering: A Tale of Sulfur Doping and Earth-Abundant CZTS Nanoparticles Sensitization. ACS Catalysis, 2017, 7, 8077-8089.	5.5	39
84	Efficient fouling control using outer-selective hollow fiber thin-film composite membranes for osmotic membrane bioreactor applications. Bioresource Technology, 2019, 282, 9-17.	4.8	39
85	Carbon nanotubes as an auxiliary catalyst in heterojunction photocatalysis for solar hydrogen. Applied Catalysis B: Environmental, 2013, 142-143, 647-653.	10.8	35
86	Electrocatalytic activities of Sb-SnO2 and Bi-TiO2 anodes for water treatment: Effects of electrocatalyst composition and electrolyte. Catalysis Today, 2017, 282, 57-64.	2.2	35
87	Plasmonic gold nanoparticle-decorated BiVO ₄ /ZnO nanowire heterostructure photoanodes for efficient water oxidation. Catalysis Science and Technology, 2018, 8, 3759-3766.	2.1	34
88	Trilayer CdS/carbon nanofiber (CNF) mat/Pt-TiO2 composite structures for solar hydrogen production: Effects of CNF mat thickness. Applied Catalysis B: Environmental, 2016, 196, 216-222.	10.8	32
89	Enhancement of Hydrogen Evolution from Water Photocatalysis Using Liquid Phase Plasma on Metal Oxide-Loaded Photocatalysts. ACS Sustainable Chemistry and Engineering, 2017, 5, 3659-3666.	3.2	32
90	High-Efficiency Solar Desalination Accompanying Electrocatalytic Conversions of Desalted Chloride and Captured Carbon Dioxide. ACS Sustainable Chemistry and Engineering, 2019, 7, 15320-15328.	3.2	32

#	Article	IF	CITATIONS
91	Electrocatalytic arsenite oxidation in bicarbonate solutions combined with CO2 reduction to formate. Applied Catalysis B: Environmental, 2020, 265, 118607.	10.8	31
92	Activation of a highly oriented columnar structure of ZnFe2O4 for photoelectrochemical water splitting: Orchestrated effects of two-step quenching and Sn4+ diffusion. Solar Energy Materials and Solar Cells, 2018, 187, 207-218.	3.0	29
93	Homogeneous photoconversion of seawater uranium using copper and iron mixed-oxide semiconductor electrodes. Applied Catalysis B: Environmental, 2017, 207, 35-41.	10.8	27
94	Analytical pyrolysis reaction characteristics of Porphyra tenera. Algal Research, 2018, 32, 60-69.	2.4	27
95	Sunlight-harnessing and storing heterojunction TiO2/Al2O3/WO3 electrodes for night-time applications. RSC Advances, 2013, 3, 17551.	1.7	26
96	CdS-loaded flexible carbon nanofiber mats as a platform for solar hydrogen production. International Journal of Hydrogen Energy, 2015, 40, 136-145.	3.8	25
97	ZnO nanostructure electrodeposited on flexible conductive fabric: A flexible photo-sensor. Sensors and Actuators B: Chemical, 2017, 240, 1106-1113.	4.0	25
98	Photoelectrochemical hydrogen production on silicon microwire arrays overlaid with ultrathin titanium nitride. Journal of Materials Chemistry A, 2016, 4, 14008-14016.	5.2	24
99	Synthesis of Aliphatic Acids from CO ₂ and Water at Efficiencies Close to the Photosynthesis Limit Using Mixed Copper and Iron Oxide Films. ACS Energy Letters, 2019, 4, 2075-2080.	8.8	24
100	Temperature-boosted photocatalytic H2 production and charge transfer kinetics on TiO2 under UV and visible light. Photochemical and Photobiological Sciences, 2016, 15, 1247-1253.	1.6	23
101	Sulfur-containing air pollutants as draw solution for fertilizer drawn forward osmosis desalination process for irrigation use. Desalination, 2017, 424, 1-9.	4.0	23
102	Mo-doped BiVO4 nanotextured pillars as efficient photoanodes for solar water splitting. Journal of Alloys and Compounds, 2017, 726, 1138-1146.	2.8	23
103	Reduced titania nanorods and Ni–Mo–S catalysts for photoelectrocatalytic water treatment and hydrogen production coupled with desalination. Applied Catalysis B: Environmental, 2021, 284, 119745.	10.8	23
104	Electrocatalytic water treatment using carbon nanotube filters modified with metal oxides. Environmental Science and Pollution Research, 2019, 26, 1036-1043.	2.7	22
105	Evaluating the Catalytic Effects of Carbon Materials on the Photocatalytic Reduction and Oxidation Reactions of TiO ₂ . Bulletin of the Korean Chemical Society, 2013, 34, 1137-1144.	1.0	22
106	Photoactive component-loaded Nafion film as a platform of hydrogen generation: Alternative utilization of a classical sensitizing system. Journal of Photochemistry and Photobiology A: Chemistry, 2009, 203, 112-118.	2.0	21
107	High efficiency solar chemical conversion using electrochemically disordered titania nanotube arrays transplanted onto transparent conductive oxide electrodes. Applied Catalysis B: Environmental, 2018, 226, 194-201.	10.8	21
108	Irradiation of liquid phase plasma on photocatalytic decomposition of acetic acid-containing wastewater over metal oxide photocatalysts. Catalysis Today, 2018, 307, 131-139.	2.2	20

#	Article	IF	CITATIONS
109	Computational density functional theory study on the selective conversion of CO2 to formate on homogeneously and heterogeneously mixed CuFeO2 and CuO surfaces. Catalysis Today, 2019, 335, 345-353.	2.2	20
110	Electrocatalytic activity of metal-doped SnO2 for the decomposition of aqueous contaminants: Ta-SnO vs. Sb-SnO. Chemical Engineering Journal, 2021, 409, 128175.	6.6	20
111	Structural Evolution of Chemically-Driven RuO2 Nanowires and 3-Dimensional Design for Photo-Catalytic Applications. Scientific Reports, 2015, 5, 11933.	1.6	19
112	Photoelectrochemical Performances of Hematite (αâ€ <scp>Fe₂O₃</scp>) Films Doped with Various Metals. Bulletin of the Korean Chemical Society, 2015, 36, 1487-1494.	1.0	19
113	Solar hydrogen peroxide production on carbon nanotubes wired to titania nanorod arrays catalyzing As(III) oxidation. Applied Catalysis B: Environmental, 2019, 252, 55-61.	10.8	19
114	Enhancing electrochemical degradation of phenol at optimum pH condition with a Pt/Ti anode electrode. Environmental Technology (United Kingdom), 2020, 41, 3248-3259.	1.2	19
115	Characterization of Ga-doped ZnO Nanorods Synthesized via Microemulsion Method. Journal of Materials Science and Technology, 2013, 29, 39-43.	5.6	18
116	Theoretical insight into effect of cation–anion pairs on CO2 reduction on bismuth electrocatalysts. Applied Surface Science, 2020, 532, 147459.	3.1	18
117	Highly efficient hydrogen production using p-Si wire arrays and NiMoZn heterojunction photocathodes. Applied Catalysis B: Environmental, 2017, 217, 615-621.	10.8	17
118	In Situ-Generated Reactive Oxygen Species in Precharged Titania and Tungsten Trioxide Composite Catalyst Membrane Filters: Application to As(III) Oxidation in the Absence of Irradiation. Environmental Science & Technology, 2020, 54, 9601-9608.	4.6	17
119	Effects of p- and d-block metal co-substitution on the electronic structure and physicochemical properties of InMO4 (M=Nb and Ta) semiconductors. Chemical Physics Letters, 2007, 434, 251-255.	1.2	16
120	Novel complexation between ferric ions and nonionic surfactants (Brij) and its visible light activity for CCl4 degradation in aqueous micellar solutions. Journal of Photochemistry and Photobiology A: Chemistry, 2004, 165, 43-50.	2.0	14
121	Substitution effect of pentavalent bismuth ions on the electronic structure and physicochemical properties of perovskite-structured Ba(In0.5Ta0.5â°xBix)O3 semiconductors. Materials Research Bulletin, 2007, 42, 1914-1920.	2.7	14
122	Facile Electrochemical Synthesis of Highly Efficient Copper–Cobalt Oxide Nanostructures for Oxygen Evolution Reactions. Journal of the Electrochemical Society, 2020, 167, 026510.	1.3	14
123	An organometal halide perovskite photocathode integrated with a MoS ₂ catalyst for efficient and stable photoelectrochemical water splitting. Journal of Materials Chemistry A, 2021, 9, 22291-22300.	5.2	14
124	Standalone photoconversion of CO2 using Ti and TiOx-sandwiched heterojunction photocatalyst of CuO and CuFeO2 films. Applied Catalysis B: Environmental, 2021, 288, 119985.	10.8	14
125	Carbon-catalyzed dye-sensitization for solar hydrogen production. Catalysis Today, 2014, 230, 15-19.	2.2	13
126	Harnessing and storing visible light using a heterojunction of WO3 and CdS for sunlight-free catalysis. Photochemical and Photobiological Sciences, 2016, 15, 1006-1011.	1.6	13

#	Article	IF	CITATIONS
127	Characterization of Bimetallic Fe-Ru Oxide Nanoparticles Prepared by Liquid-Phase Plasma Method. Nanoscale Research Letters, 2016, 11, 344.	3.1	12
128	ZnO rods rooted on manifold carbon nanofiber paper as a scalable photocatalyst platform: the effects of ZnO morphology. RSC Advances, 2016, 6, 85521-85528.	1.7	12
129	Effect of liquid phase plasma on photocatalysis of water for hydrogen evolution. International Journal of Hydrogen Energy, 2017, 42, 17386-17393.	3.8	12
130	Photocatalytic H ₂ production on trititanate nanotubes coupled with CdS and platinum nanoparticles under visible light: revisiting H ₂ production and material durability. Faraday Discussions, 2017, 198, 419-431.	1.6	12
131	Effects of electrochemical synthetic conditions on surface property and photocatalytic performance of copper and iron-mixed p-type oxide electrodes. Journal of Materials Science and Technology, 2018, 34, 1503-1510.	5.6	12
132	Fouling and performance of outer selective hollow fiber membrane in osmotic membrane bioreactor: Cross flow and air scouring effects. Bioresource Technology, 2020, 295, 122303.	4.8	12
133	Effect of ZnO Electrodeposited on Carbon Film and Decorated with Metal Nanoparticles for Solar Hydrogen Production. Journal of Materials Science and Technology, 2016, 32, 1059-1065.	5.6	11
134	Photoelectrochemical hydrogen production using CdS nanoparticles photodeposited onto Li-ion-inserted titania nanotube arrays. Catalysis Today, 2018, 303, 289-295.	2.2	11
135	Electrocatalytic cogeneration of reactive oxygen species for synergistic water treatment. Chemical Engineering Journal, 2019, 358, 497-503.	6.6	11
136	Assembling a supercapacitor electrode with dual metal oxides and activated carbon using a liquid phase plasma. Journal of Environmental Management, 2017, 203, 880-887.	3.8	10
137	Bowmanella dokdonensis sp. nov., a novel exoelectrogenic bacterium isolated from the seawater of Dokdo, Korea. Antonie Van Leeuwenhoek, 2016, 109, 907-914.	0.7	9
138	The effect of nanostructure dimensionality on the photoelectrochemical properties of derived TiO2 films. Electrochimica Acta, 2021, 373, 137900.	2.6	9
139	Effect of shape-driven intrinsic surface defects on photocatalytic activities of titanium dioxide in environmental application. Applied Surface Science, 2017, 423, 71-77.	3.1	7
140	Computational characterization of nitrogen-doped carbon nanotube functionalized by Fe adatom and Fe substituent for oxygen reduction reaction. Applied Surface Science, 2019, 485, 342-352.	3.1	7
141	Electrocatalytic activities of electrochemically reduced tubular titania arrays loaded with cobalt ions in flow-through processes. Chemical Engineering Journal, 2021, 404, 126410.	6.6	7
142	Synergistic effect of Sn doping and hydrogenation on hematite electrodes for photoelectrochemical water oxidation. Materials Chemistry Frontiers, 2021, 5, 6592-6602.	3.2	7
143	Microporous Zeolites as Catalysts for the Preparation of Decyl Glucoside from Glucose with 1-Decanol by Direct Glucosidation. Catalysts, 2016, 6, 216.	1.6	6
144	Molecular catalysts for artificial photosynthesis: general discussion. Faraday Discussions, 2017, 198, 353-395.	1.6	6

#	Article	IF	CITATIONS
145	Sunlight-charged heterojunction TiO2 and WO3 particle-embedded inorganic membranes for night-time environmental applications. Photochemical and Photobiological Sciences, 2018, 17, 491-498.	1.6	6
146	Enhanced Charge Transfer Process in Morphology Restructured TiO ₂ Nanotubes via Hydrochloric Acid Assisted One Step <i>In‧itu</i> Hydrothermal Approach. ChemCatChem, 2019, 11, 5606-5614.	1.8	6
147	Platinum-decorated Cu(InGa)Se2/CdS photocathodes: Optimization of Pt electrodeposition time and pH level. Journal of Alloys and Compounds, 2017, 692, 294-300.	2.8	5
148	Water industry: water-energy-health nexus. Environmental Science and Pollution Research, 2019, 26, 1013-1014.	2.7	5
149	Exploring the photoelectrocatalytic behavior of free-standing TiO2 nanotube arrays on transparent conductive oxide electrodes: Irradiation direction vs. alignment direction. Catalysis Today, 2019, 335, 319-325.	2.2	5
150	Surface passivation of zinc ferrite nanorod photoanodes by spray-deposited silicon oxide layer for enhanced solar water splitting. Journal of the Taiwan Institute of Chemical Engineers, 2020, 107, 89-97.	2.7	5
151	Correlations among defect type, photoconductivity and photoreactivity of doped TiO2. Korean Journal of Chemical Engineering, 2001, 18, 873-878.	1.2	4
152	Effect of Fe/N-doped carbon nanotube (CNT) wall thickness on CO2 conversion: A DFT study. Sustainable Materials and Technologies, 2020, 26, e00224.	1.7	3
153	Facile thermochemical conversion of FeOOH nanorods to ZnFe2O4 nanorods for high-rate lithium storage. RSC Advances, 2019, 9, 21444-21450.	1.7	2
154	Optimizing RuOxâ^TiO2 composite anodes for enhanced durability in electrochemical water treatments. Chemosphere, 2021, 265, 129166.	4.2	2
155	Catalysis for water purification. Catalysis Today, 2017, 282, 1.	2.2	1